Supplementary Table 1. Cell proliferation index in *K14-Cre;Shh$^{c/n}$* and control palatal shelves at E13.5.

	1	2	3	4
CK-PE	**0.3696±0.03910**	**0.3728±0.03530**	**0.3727±0.02652**	**0.3466±0.02205**
MT-PE	****0.1968±0.03670**	**0.3929±0.02548**	****0.3261±0.01549**	**0.3540±0.02367**
CK-PM	**0.3221±0.02357**	**0.3981±0.05611**	**0.4002±0.03461**	**0.4162±0.05256**
MT-PM	**0.3018±0.03391**	**0.4100±0.05984**	****0.3153±0.03648**	****0.2135±0.02806**

** denotes the mutant samples with significant difference in cell proliferation index from the control samples ($p < 0.05$). Data were expressed as ratios of BrdU labeled nuclei to total cell nuclei ± standard deviation. Data were recorded from 10 continuous frontal sections through the E13.5 palatal shelves anterior to the maxillary first molar tooth germs in comparable positions in control and *K14-Cre;Shh$^{c/n}$* mutant embryos. CK-PE, control palatal epithelium; MT-PE, *K14-Cre;Shh$^{c/n}$* mutant palatal epithelium; CK-PM, control palatal mesenchyme; MT-PM, mutant palatal mesenchyme.

Supplementary Figure Legends:

Supplementary Figure 1. Tissue specificity of Cre mediated activation of *lacZ* expression in the developing craniofacial complex of *Osr2-IresCre;R26R* embryos at E12.5. X-gal staining on frontal sections from the anterior (A), middle (B) and posterior (C) palate regions is shown. LacZ activity was detected throughout the anterior-posterior axis of the developing palatal mesenchyme, indicating strong Cre activity from the onset of palatal outgrowth. In addition, lacZ activity was detected in a subset of the nasal mesenchyme, in a subset of mesenchymal cells underlying the epithelium in the developing tongue, in the developing eyelid epithelium and mesenchyme (arrows in B and C), in the lateral maxillary and mandibular mesenchyme, and in the mandibular mesenchyme flanking the base of the developing tongue. No lacZ activity was detected in the developing brain. Some lacZ activity was also detected in the thin mesenchymal layer surrounding the developing brain at this stage (arrowheads in B and C). br, brain; e, eye; man, mandible; max, maxilla; n, nasal septum; p, palatal shelf; t, tongue.

Supplementary Figure 2. Highly specific down-regulation of expression of *Ptch1*, *Gli1*, and *Fgf10* in the developing eyelid and palate in E13 *Osr2-IresCre;Smo*$^{c/c}$ mutant embryos. (A, B) Compared with the control embryo (A), *Osr2-IresCre;Smo*$^{c/c}$ mutant embryo (B) had dramatic down-regulation of *Ptch1* expression in the palatal mesenchyme and in the eyelid epithelium and mesenchyme. In contrast, expression of *Ptch1* in the ventral diencephalon (arrowheads in A and B) and in the mandibular osteoblasts next to the Meckel's cartilage was not significantly different in the control and *Osr2-IresCre;Smo*$^{c/c}$ mutant littermates. Insets in A and B show

higher magnification views of *Ptch1* expression in the developing upper eyelids (arrows) of the control and *Osr2-IresCre;Smo*$^{c/c}$ mutant embryos, respectively. (C, D) Similar to that of *Ptch1*, expression of *Gli1* was also highly specifically downregulated in the developing palatal mesenchyme and eyelid tissues (arrows) in the *Osr2-IresCre;Smo*$^{c/c}$ mutant embryos (D), compared with the control littermates (C). (E, F) *Fgf10* expression is down-regulated in the developing palatal and eyelid mesenchyme in *Osr2-IresCre;Smo*$^{c/c}$ mutant embryos (F), in comparison with the control littermates (E). Expression of *Fgf10* in the control embryos (E) overlapped with that of *Ptch1* (A) and of *Gli1* (C) in the developing palatal shelves and eyelids. In contrast, strong *Fgf10* expression in the mesenchyme behind the developing eyes (arrows in E and F) and in the mandibular mesenchyme surrounding the Meckel's cartilage was unaffected in the *Osr2-IresCre;Smo*$^{c/c}$ mutant embryos (F), compared with the control littermates (E). Insets in E and F show higher magnification views of the *Fgf10* expression in the developing upper eyelids (arrowheads) of control and *Osr2-IresCre;Smo*$^{c/c}$ mutant littermates, respectively. e, eye; mc, Meckel's cartilage; p, palatal shelves; t, tongue.

Supplementary Figure 3. Comparison of *Bmp2* (A, B) and *Bmp4* (C, D) mRNA expression in the craniofacial tissues in the *Osr2-IresCre;Smo*$^{c/+}$ (A, C) and *Osr2-IresCre;Smo*$^{c/c}$ mutant (B, D) embryos. Arrowheads point to the medial edge of the anterior palatal shelves. Both *Bmp2* and *Bmp4* are expressed abundantly in multiple tissues in the craniofacial region, including in the medial nasal, lateral nasal, maxillary and mandibular processes. Limited expression of *Bmp2* and *Bmp4* mRNA was detected in the medial edge palatal mesenchyme in the control embryos. *Bmp2* expression in the palatal mesenchyme was downregulated whereas *Bmp4*

expression in the anterior palatal mesenchyme was expanded in the *Osr2-IresCre;Smo*$^{c/c}$ mutant embryos (B, D). man, mandible; max, maxilla; n, nasal septum; p, palatal shelf; t, tongue.

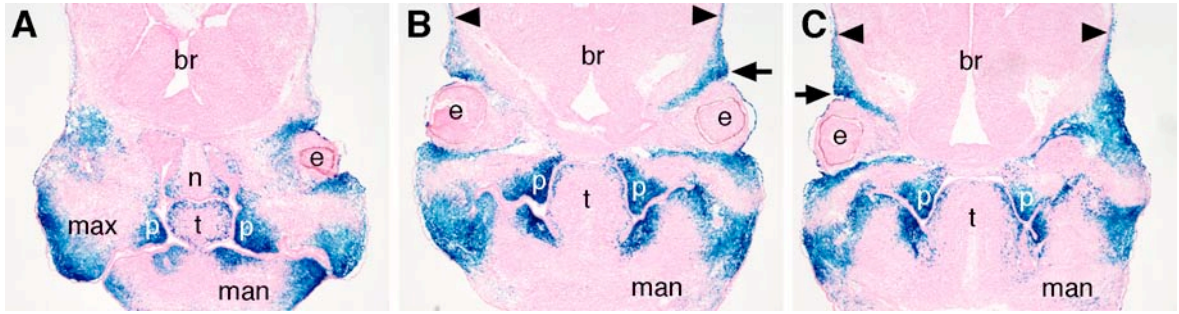

Fig. S1

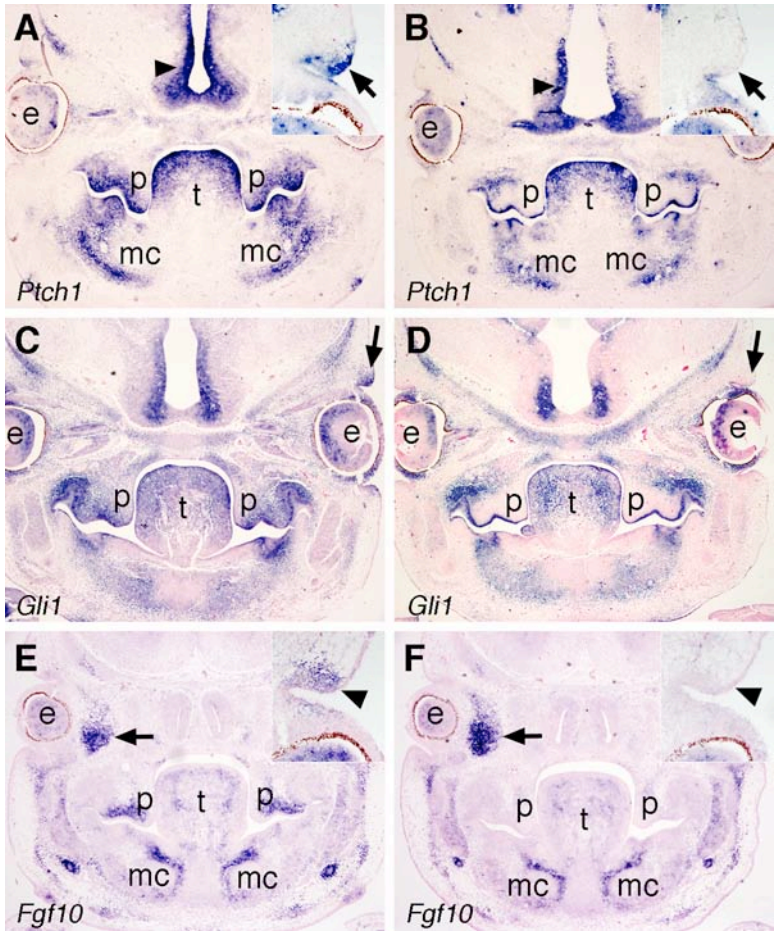
A
e
p
t
p
mc
mc
Ptch1
B
e
p
t
p
mc
mc
Ptch1
C
e
e
p
t
p
Gli1
D
e
e
p
t
p
Gli1
E
e
p
t
p
mc
mc
Fgf10
F
e
p
t
p
mc
mc
Fgf10

Fig. S2

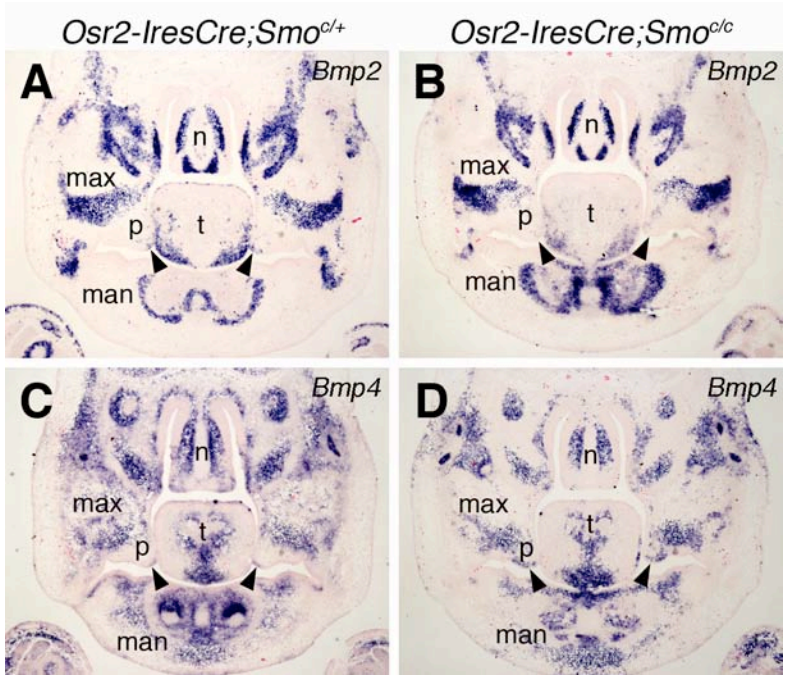
Osr2-IresCre;Smo^c/+
Osr2-IresCre;Smo^c/c
A
Bmp2
n
max
p
t
man
B
Bmp2
n
max
p
t
man
C
Bmp4
n
max
p
t
man
D
Bmp4
n
max
t
p
man

Fig. S3